Title
Adiabatic beam dynamics in a modified betatron

Journal
Physics of Fluids, 28(6)

ISSN
00319171

Authors
Roberts, G. A
Rostoker, N.

Publication Date
1985

DOI
10.1063/1.865374

Adiabatic beam dynamics in a modified betatron

G. A. Roberts and N. Rostoker
Department of Physics, University of California, Irvine, California 92717

(Received 5 October 1984; accepted 18 January 1985)

Electron beams in modified betatrons were previously analyzed by using a paraxial treatment. This treatment is valid only for a beam where particles have an axial velocity much larger than their perpendicular velocity. However, in accelerators such as the UCI Modified Betatron, the beam does not satisfy the paraxial assumption. Another treatment based on the guiding center equations is presented. In this treatment the paraxial assumption is not necessary. Corrections to the conventional "betatron condition" are found and compared with recent experiments. Additionally, this treatment can describe nonparaxial quasiconfined particles. The effect of these quasiconfined particles is examined, and it is shown that they provide fields that are necessary to stabilize the beam.

I. INTRODUCTION

A high-current accelerator that has received some attention recently is the modified betatron. A cut-away view of the modified betatron is shown in Fig. 1. It is basically a conventional betatron with a toroidal magnetic field. Previous treatments of the modified betatron[1,2] were based on the paraxial assumption. These treatments only apply to beams where the perpendicular velocity ($v_\perp$) is small with respect to the axial beam velocity (v_z) and are reasonable for accelerators that use tangential injection schemes such as that proposed by the Naval Research Laboratory group.[3] However, for inductive charging injection, such as that used on the UCI Modified Betatron,[4,5] the assumption that $v_\perp^2 \ll v_z^2$ is not reasonable. Specifically, with this injection method the electron source is thermionic so electrons are emitted in various directions, and there is a fast magnetic compression. Also, the paraxial assumption is not valid for particles that are trapped in quasiconfined orbits. As in tokamaks, it is expected that many of the particles in the betatron are in banana-like orbits that do not go around the torus.

Instead of making a treatment based on the paraxial assumption ($v_\perp^2 \ll v_z^2$), a treatment has been developed based on the guiding center approach. The adiabatic guiding center equation is valid when the fields change slowly during a cyclotron orbit so that $|a_c(\partial B_i/\partial x_j)| \ll |\mathbf{B}| \equiv B$ and $|(1/\Omega)(\partial B/\partial t)| \ll B$, where a_c is the cyclotron radius and Ω is the cyclotron frequency: $eB/\gamma mc$. With a large toroidal magnetic field, the guiding center approximation should be valid.

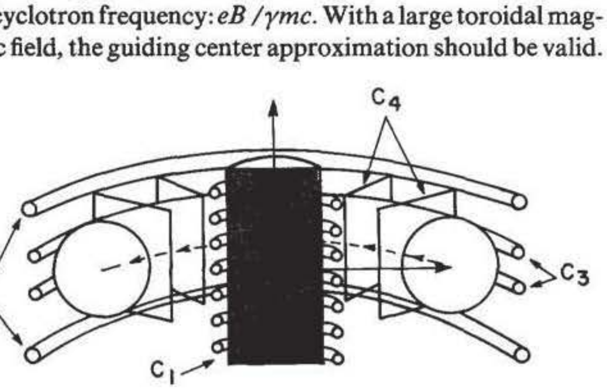

FIG. 1. The modified betatron. Increasing current in the C_1 coil will create an electric field that will accelerate the beam. C_2 coils produce the betatron field which, in a conventional betatron, will balance the beam's centrifugal force. C_3 coils can trim the betatron field. C_4 coils produce the toroidal magnetic field.

In Sec. II a procedure using averages of the guiding center equation to find the beam motion is described. The stabilizing effects of quasiconfined particles that are trapped by toroidal field anomalies are discussed in Sec. III. In Sec. IV a comparison of the paraxial and guiding center treatments is presented.

II. GUIDING CENTER EQUATIONS

In accelerators like the UCI Modified Betatron, the toroidal magnetic field is initially much larger than all other fields. A treatment that is applicable to a large magnetic field is the guiding center treatment. In this treatment the particles within a beam will essentially follow the magnetic field lines. The electric field and curvature of the magnetic field lines will cause drifts.

In the guiding center treatment the particle motion is assumed to consist of guiding center motion denoted by $\mathbf{R}$ and a fast gyromotion denoted by $\mathbf{a}$:

$$\mathbf{r} = \mathbf{R} + \mathbf{a} = \mathbf{R} - (\gamma mc/eB^2)(\mathbf{B}\times\mathbf{v}), \tag{1}$$

where $\mathbf{r}$ is the particle position, $\mathbf{v}$ is the particle velocity, and $\mathbf{B}$ is the magnetic field. The guiding center drift velocity equation can be obtained by differentiating the above with respected to time, using the Lorentz force to replace $\dot{\mathbf{v}}$, assuming the fields are static during a gyro-orbit, and averaging over the cyclotron motion.

$$\dot{\mathbf{R}} = \mathbf{V}_\parallel + \frac{c(\mathbf{E}\times\mathbf{B})}{B^2} - \frac{\gamma mc}{eB^2}\frac{(\mathbf{n}\times\mathbf{B})}{R}\left(V_\parallel^2 + \frac{1}{2}V_\perp^2\right), \tag{2}$$

where $\mathbf{n} = -R(\hat{b}\cdot\nabla)\hat{b}$, $\mathbf{V}_\perp = \langle(\hat{b}\times\mathbf{v})\times\hat{b}\rangle$, $\mathbf{V}_\parallel \cong [(\mathbf{v}\cdot\mathbf{B})/B^2]\mathbf{B}$, and $\hat{b} = \mathbf{B}/|\mathbf{B}|$. In order to evaluate the above equation, the external fields and the self-fields must first be determined.

As can be seen in Fig. 1, the toroidal and betatron fields can be approximated by the following:

$$\begin{aligned} B_z &\cong B_{z0}(1 + x/R), \\ B_y &\cong B_{y0}(1 + sx/R), \\ B_x &\cong (sy/R)B_{y0}, \end{aligned} \tag{3}$$

where R is the major radius of the torus, s is the betatron field index, and the coordinate system in Fig. 2 has been used. The self-electric and self-magnetic fields within the beam must also be determined. To evaluate these fields the beam was

 0031-9171/85/061968-06$01.90

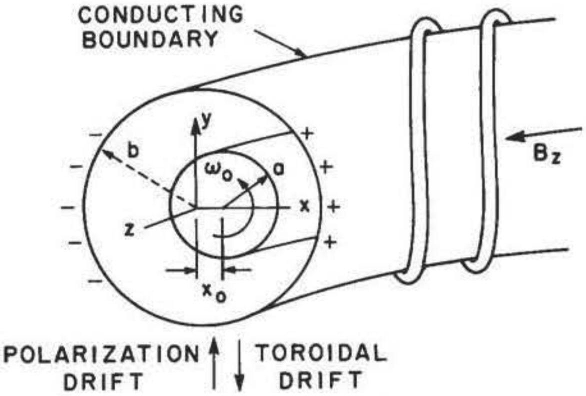

FIG. 2. Local coordinate system for toroidal geometry. Additionally, the drifts from the beam polarizing the wall and the curvature of the toroidal magnetic field are shown.

considered to be circular in cross section and of constant density. The self-fields of a constant density circular beam can be expressed as follows:

$$\mathbf{E}_s = -2\pi ne[(x - X_0)\hat{x} + (y - Y_0)\hat{y}],$$
$$\mathbf{B}_s = -2\pi ne(v_z/c)[(x - X_0)\hat{y} - (y - Y_0)\hat{x}], \tag{4}$$

where (X_0, Y_0) is the position of the center of the beam and n is the beam density. The beam will also induce currents and charge on the surrounding walls. The induced current will be neglected since in the UCI Modified Betatron the wall is slotted to eliminate the current that produces a static magnetic field. The electric field from the wall charge is approximately the following[1]:

$$\mathbf{E}_i \cong -2Ne(1/b^2)(X_0\hat{x} + Y_0\hat{y}), \tag{5}$$

where $N \equiv \pi na^2$ is the beam's line density and b is the minor radius of the torus. These fields will determine the motion of the guiding center of a particle via Eq. (2). The $\mathbf{V}_\parallel$ term in Eq. (2) is given by the following:

$$\mathbf{V}_\parallel \cong V_\parallel \left\{ \hat{z} + \left[\left(\frac{B_{y0}}{B_{z0}}\right)\frac{sy}{R} + \left(\frac{2\pi ne}{B_{z0}}\right)\left(\frac{v_z}{c}\right)(y - Y_0) \right]\hat{x} + \left[\left(\frac{B_{y0}}{B_{z0}}\right)\left(1 + \frac{(s-1)x}{R}\right) - \left(\frac{2\pi ne}{B_{z0}}\right)\left(\frac{v_z}{c}\right)(x - X_0) \right]\hat{y} \right\}. \tag{6}$$

In the above it has been assumed that $B_{z0} \gg B_{y0}$; $x, y \ll R$, $2\pi ne|\mathbf{x} - \mathbf{X}_0| \ll B_{z0}$; and $V_z \cong V_\parallel$. The $\mathbf{E}\times\mathbf{B}$ term in the guiding center equation can be determined from Eqs. (4) and (5). It is given by the following:

$$\frac{c(\mathbf{E}\times\mathbf{B})}{B^2} \cong -c\left(\frac{2\pi ne}{B_{z0}}\right)\left\{ \left[\left(\frac{a}{b}\right)^2 Y_0 + (y - Y_0) \right]\hat{x} - \left[\left(\frac{a}{b}\right)^2 X_0 + (x - X_0) \right]\hat{y} \right\}. \tag{7}$$

The curvature of the magnetic field lines ($\mathbf{n}$) must also be found to evaluate the guiding center equation. Assuming $B_{z0} \gg B_{y0}$ then $\mathbf{n}$ is given by

$$\mathbf{n} = -R(\hat{b}\cdot\nabla)\hat{b} \cong -\hat{x}. \tag{8}$$

By using Eqs. (6)–(8), the guiding center velocity $(\dot{X}, \dot{Y}, \dot{Z})$ for a particle in the beam can be expressed:

$$\dot{X} \cong -\omega_0(y - Y_0)\left[1 - \left(\frac{V_\parallel}{c}\right)^2\right] + \frac{V_\parallel B_{y0}}{B_{z0}}\frac{sy}{R} - \frac{2Nec}{b^2B_{z0}}Y_0, \tag{9}$$

$$\dot{Y} \cong \omega_0(x - X_0)\left[1 - \left(\frac{V_\parallel}{c}\right)^2\right] + \frac{V_\parallel B_{y0}}{B_{z0}}\left(1 + \frac{(s-1)x}{R}\right) - \frac{(V_\parallel^2 + \frac{1}{2}V_\perp^2)}{R\Omega_z} + \frac{2Nec}{b^2B_{z0}}X_0, \tag{10}$$

where

$$\omega_0 = \frac{\omega_p^2}{2\Omega_z}, \quad \omega_p^2 = \frac{4\pi ne^2}{\gamma m}, \quad \Omega_z = \frac{eB_{z0}}{\gamma mc}.$$

To obtain an expression for the beam motion, consider averaging the above equations over all the beam particles. In this case $\langle X\rangle = X_0$, $\langle Y\rangle = Y_0$, $\langle \dot{X}\rangle = \dot{X}_0$, and $\langle \dot{Y}\rangle = \dot{Y}_0$. Also $\langle V_\parallel x\rangle \cong \langle V_\parallel\rangle X_0$ and $\langle V_\parallel y\rangle \cong \langle V_\parallel\rangle Y_0$, since $V_\parallel$ is only weakly coupled to the particle position. After averaging these equations over the beam particles, they become the following:

$$\dot{X}_0 = \frac{\langle V_\parallel\rangle B_{y0}}{B_{z0}}\frac{sY_0}{R} - \frac{2Nec}{b^2B_{z0}}Y_0, \tag{11}$$

$$\dot{Y}_0 = \frac{\langle V_\parallel\rangle B_{y0}}{B_{z0}}\left[\left(1 + \frac{(s-1)}{R}X_0\right)\right] + \frac{2Nec}{b^2B_{z0}}X_0 - \frac{\langle V_\parallel^2\rangle + \frac{1}{2}\langle V_\perp^2\rangle}{R\Omega_z}, \tag{12}$$

where $\langle\ \ \rangle$ indicates averaging. For a coasting beam, these equations can be expressed in terms of two independent harmonic oscillators:

$$\ddot{X}_0 + \Omega^2 X_0 = F, \tag{13}$$

$$\ddot{Y}_0 + \Omega^2 Y_0 = 0, \tag{14}$$

where

$$\Omega^2 = \left(\frac{2Nec}{b^2B_{z0}} - \frac{s\langle V_\parallel\rangle B_{y0}}{B_{z0}R}\right)\left(\frac{2Nec}{b^2B_{z0}} - \frac{(1-s)\langle V_\parallel\rangle B_{y0}}{B_{z0}R}\right), \tag{15}$$

$$F = \left(\frac{2Nec}{b^2B_{z0}} - \frac{s\langle V_\parallel\rangle B_{y0}}{B_{z0}R}\right) \times \left(\frac{\langle V_\parallel^2\rangle}{R\Omega_z} - \frac{\langle V_\parallel\rangle B_{y0}}{B_{z0}} + \frac{\langle V_\perp^2\rangle}{2R\Omega_z}\right). \tag{16}$$

Equations (13) and (14) indicate that the beam will oscillate about an equilibrium position. The equilibrium position is given by the quantity F/Ω^2 and is the following:

$$\bar{X}_0 = \frac{F}{\Omega^2} = \left(\frac{\langle V_\parallel^2\rangle}{R} - \langle V_\parallel\rangle\Omega_{y0} + \frac{\langle V_\perp^2\rangle}{2R}\right) \times \left[\Omega_z\left(\frac{2Nec}{b^2B_{z0}} - \frac{(1-s)\langle V_\parallel\rangle B_{y0}}{B_{z0}R}\right)\right]^{-1}, \tag{17a}$$

or

$$0 = \frac{\langle V_\parallel^2\rangle + 1/2\langle V_\perp^2\rangle}{\Omega_z R} - \frac{\Omega_y\langle V_\parallel\rangle}{\Omega_z} \times \left(1 - \frac{(1-s)\bar{X}_0}{R}\right) - \frac{2Nec}{b^2B_{z0}}\bar{X}_0. \tag{17b}$$

Equation (17b) shows that the average beam position ($\bar{X}_0$) is determined by the x position where all drifts cancel. Specifically the first term in Eq. (17b) is from the curvature of the toroidal magnetic field. The second term is the drift caused by the particles following the betatron field and the curvature of the betatron field. The third is the drift from the beam inducing charge on the wall (polarizing). Depending on the value of $V_\parallel$ and B_{y0}, the equilibrium can have $\bar{X}_0 > 0$ or $\bar{X}_0 < 0$.

It can be seen from the above equations that if the "betatron condition" $[\langle V_\parallel \rangle = \Omega_y R = (eB_{y0}/\gamma mc)R]$ is satisfied and $V_\parallel = 0$ then $\bar{X}_0 = 0$, and the beam will oscillate about the center of the chamber. However, Eq. (17a) indicates a modification of the "betatron condition":

$$\Omega_y R = \frac{\langle V_\parallel^2 \rangle + \frac{1}{2}\langle V_\perp^2 \rangle}{\langle V_\parallel \rangle}. \tag{18}$$

This condition differs from the usual "betatron condition" because of the inclusion of $V_\perp$. In the UCI Betatron it was found that, to trap a beam, $\Omega_y R$ had to be about three to four times larger than the maximum velocity that a particle could have during injection ($\sqrt{2\, eV_0/m}$, where V_0 is the injector voltage). Equation (18) can reconcile this by assuming a large $V_\perp$ which is reasonable considering the method of injection and the magnetic compression. Additionally, Eqs. (13) and (14) indicate that unless $s = 1/2$, Ω^2 will become negative for some particular range of $\langle V_\parallel \rangle$ and B_{y0}. This corresponds to an instability. The paraxial treatment also indicates the same instability.[6]

In the UCI Modified Betatron the beam was accelerated and eventually hit the outer wall. The final electron momentum inferred from x-ray energy measurments was about $0.5eB_y R/c$ so that $\langle V_\parallel \rangle R\Omega_{y0} \cong 2\langle V_\parallel^2 \rangle$. With this information, Eq. (17a) indicates a beam equilibrium deflection that would indeed take the beam to the outer wall. For $I = 150$ A, $\langle \gamma - 1 \rangle mc^2 = 500$ keV, $\langle V_\parallel \rangle = 2.6 \times 10^{10}$ cm/sec, $N = I/e\langle V_\parallel \rangle = 3.6 \times 10^{10}\ \mathrm{cm}^{-1}$, $b = 5$ cm, $B_{y0} = 130$ G, $B_{z0} = 4$ kG, $s = 0.8$, and $R = 40$ cm, Eq. (17) predicts $X_0 = -76$ cm. The sign indicates a deflection to the outer wall but the magnitude is too large. This and other discrepancies can be accounted for by considering a large number of quasiconfined electrons that form a background beam.

III. TWO-BEAM TREATMENT

To obtain a closer correspondence to the experiment, it was postulated that there were a large number of electrons in quasiconfined orbits which did not get accelerated. Electrons in such orbits have previously been postulated to explain experiments at Maxwell Laboratories.[7] In the betatron experiments at UCI, electrostatic probes see two basic frequencies. One is a high frequency and the other is a low frequency. If the frequencies are interpreted in terms of diocotron oscillations then the fast frequency corresponds to a line density of $10^{12}\ \mathrm{cm}^{-1}$ and the slow frequency corresponds to a line density of about $10^{10}\ \mathrm{cm}^{-1}$. Current measurements indicate that the beam has a density that corresponds to that predicted by the low frequency. The high frequency is attributed to a large number of nonaccelerated quasiconfined particles. Particles should be trapped in nonaccelerating orbits if $\mu(\partial B/\partial z) > eE_z$ where E_z is the accelerating toroidal electric field and $\mu = \frac{1}{2} mV_\perp^2/B$. In the betatron, $E_z \sim 0.8$ V/cm, so if it is assumed that B changes about 1% over $L = 10$ cm, then the requirement for particles to be in these nonaccelerating orbits is

$$\tfrac{1}{2} mV_\perp^2/e > E_z L(B/\Delta B) \sim 10^3\ \mathrm{V}. \tag{19}$$

Considering the method of injection where the voltage applied to the injector is greater than 10^4 V, and the magnetic compression, most of the electrons will have sufficient perpendicular energy to remain trapped between local mirrors provided that they are not in the loss cone ($V_\parallel^2 \ll V_\perp^2$).

In light of the possibility of large numbers of quasiconfined particles, consider the accelerator to have two beams. One beam consists of nonaccelerated trapped particles, and the other is the accelerated beam. The background beam will supply fields that are necessary to stabilize the accelerated beam. In this model, consider a background beam of radius a', density n', and position (X'_0, Y'_0), in addition to an accelerated beam, as seen in Fig. 3. To find the motion of these beams, first consider the motion of the particles in the beams. The particles in the accelerated beam will experience all the previously described fields in addition to the background beam self-fields (E'_s, B'_s) and induced electric field (E'_i). These fields are given by the following:

$$\mathbf{E}'_s = -2\pi n' e[(x - X'_0)\hat{x} + (y - Y'_0)\hat{y}], \tag{20}$$

$$\mathbf{B}'_s = -2\pi n' e(V'_\parallel/c)[(x - X'_0)\hat{y} - (y - Y'_0)\hat{x}] \cong 0, \tag{21}$$

$$\mathbf{E}'_i = -(2N'e/b^2)(X'_0\hat{x} + Y'_0\hat{y}), \tag{22}$$

where it has been assumed that the background beam has a constant density profile. Similarly, the particles in the background beam will experience the background beam fields and the accelerated beam's self- and induced fields which are the following:

$$\mathbf{E}_s = \begin{cases} -2\pi ne((x' - X_0)\hat{x} + (y' - Y_0)\hat{y}) & |\mathbf{x}' - \mathbf{X}_0| < a, \\ \dfrac{-2\pi nea^2((x' - X_0)\hat{x} + (y' - Y_0)\hat{y})}{|(x' - X_0)\hat{x} + (y' - Y_0)\hat{y}|^2} & |\mathbf{x}' - \mathbf{X}_0| > a, \end{cases} \tag{23}$$

$$\mathbf{B}_s = \begin{cases} -2\pi ne(v_\parallel/c)((x' - X_0)\hat{y} - (y' - Y_0)\hat{x}) \\ |\mathbf{x}' - \mathbf{X}_0| < a, \\ \dfrac{-2\pi nea^2(v_\parallel c)((x' - X_0)\hat{y} - (y' - Y_0)\hat{x})}{|(x' - X_0)\hat{x} + (y' - Y_0)\hat{y}|^2} \\ |\mathbf{x}' - \mathbf{X}_0| > a, \end{cases} \tag{24}$$

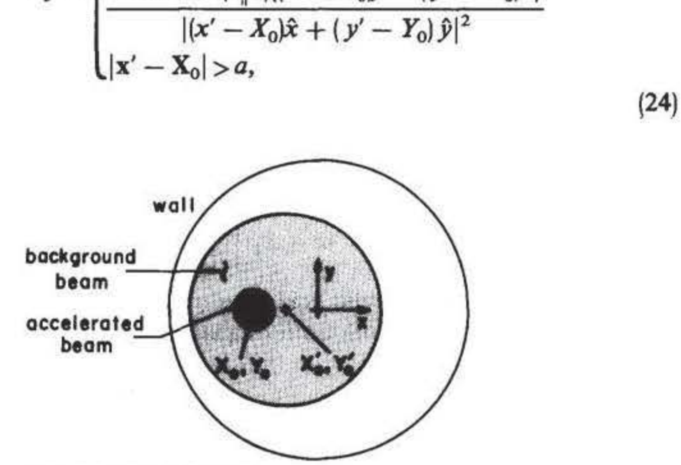

FIG. 3. Two-beam model.

$$\mathbf{E}_i = (2Ne/b^2)(X_0\hat{x} + Y_0\hat{y}). \tag{25}$$

The guiding center of the accelerated beam particles and the background beam particles can be obtained by substituting the expressions for the fields into Eq. (2). When this is done the following equations are obtained for the accelerated beam particles:

$$\dot{X} = -\omega_0(y - Y_0)[1 - (V_\parallel/c)^2] - \omega_0'(y - Y_0') - (2Nec/b^2B_{z0})Y_0 - \frac{2N'ec}{b^2B_{z0}}Y_0' + \frac{sV_\parallel B_{y0}}{B_{z0}}\left(\frac{y}{R}\right), \tag{26}$$

$$\dot{Y} = \omega_0(x - X_0)[1 - (V_\parallel/c)^2] + \omega_0'(x - X'_0) + (2Nec/b^2B_{z0})X_0 + \frac{2N'ec}{b^2B_{z0}}X_0' + \frac{V_\parallel B_{y0}}{B_{z0}}\left(1 + \frac{(s-1)x}{R}\right) - \frac{(V_\parallel^2 + \frac{1}{2}V_\perp^2)}{\Omega_z R}, \tag{27}$$

where $\omega_0' = \omega_p'^2/2\Omega_z$ and it has been assumed that $V_\parallel'/c \ll 1$. In the same manner the guiding center of the background beam particles can be obtained:

$$\dot{X}' = -\omega_0'(y' - Y_0') - \omega_0(y' - Y_0)\theta(a - |\mathbf{x}' - \mathbf{X}_0|) - \omega_0\theta(|\mathbf{x}' - \mathbf{X}_0| - a)\left(\frac{a^2(y' - Y_0)}{|\mathbf{x}' - \mathbf{X}_0|^2}\right) - \frac{2N'ec}{b^2B_{z0}}Y_0' - \frac{2Nec}{b^2B_{z0}}Y_0 + \frac{sV_\parallel' B_{y0}}{B_{z0}}\left(\frac{y'}{R}\right), \tag{28}$$

$$\dot{Y}' = \omega_0'(x' - X_0') + \omega_0\theta(a - |\mathbf{x}' - \mathbf{X}_0|)(x' - X_0) + \omega_0\theta(|\mathbf{x}' - \mathbf{X}_0| - a)\left(\frac{a^2(x' - X_0)}{|\mathbf{x}' - \mathbf{X}_0|^2}\right) + \frac{2N'ec}{b^2B_{z0}}X_0' + \frac{2Nec}{b^2B_{z0}}X_0 + \frac{V_\parallel' B_{y0}}{B_{z0}}\left(1 + \frac{(s-1)x'}{R}\right) - \frac{(V_\parallel'^2 + \frac{1}{2}V_\perp'^2)}{\Omega_z R}, \tag{29}$$

where

$$\theta(\xi) = \begin{cases} 1 & \xi > 0, \\ 0 & \xi < 0. \end{cases}$$

The beam equations can be obtained by averaging the particle guiding center equations. In the background beam, $\langle V_\parallel' \rangle = 0$, $\langle x' \rangle = X_0'$, and $\langle y' \rangle = Y_0'$. Futhermore, it is assumed that the motion of the background beam in the direction parallel to the magnetic field is weakly coupled to the motion in the perpendicular directions, so that $\langle V_\parallel' x' \rangle = \langle V_\parallel' \rangle\langle x' \rangle = 0$ and $\langle V_\parallel' y' \rangle = \langle V_\parallel' \rangle\langle y' \rangle = 0$. The terms representing the action of the accelerated beam self-fields on the background beam particles require nontrivial averaging. For a constant density beam the average of any function of $\mathbf{x}'[\equiv g(\mathbf{x}')]$, such as the quantity in question, is just the spatial average of $g(\mathbf{x}')$ over the beam area. This can be shown by assuming a distribution function $f(\mathbf{x}',\mathbf{v}')$ in which case $\langle g \rangle$ is the following:

$$\langle g \rangle = \int d\mathbf{x}'\, g(\mathbf{x}')\left(\int d\mathbf{v}' f(\mathbf{x}',\mathbf{v}')\right) = \frac{1}{A}\int_A d\mathbf{x}'\, g(\mathbf{x}'), \tag{30}$$

where A is the area of the beam. Using this, consider the regions in Fig. 4. The drifts from the accelerated beam self-electric field for each of the regions within the background beam are the following:

$$\mathbf{V}_{\mathrm{I}} = -\omega_0[(y' - Y_0)\hat{x} - (x' - X_0)\hat{y}],$$

$$\mathbf{V}_{\mathrm{II}} = \mathbf{V}_{\mathrm{III}} = -\omega_0(a^2/|\mathbf{x}' - \mathbf{X}_0|^2)[(y' - Y_0)\hat{x} - (x' - X_0)\hat{y}], \tag{31}$$

where $\mathbf{V}_{\mathrm{I}}$, $\mathbf{V}_{\mathrm{II}}$, and $\mathbf{V}_{\mathrm{III}}$ are the drifts in regions I, II, and III, respectively. When the drift in region I is averaged over region I it will vanish since $\langle y' \rangle = Y_0$ and $\langle x' \rangle = X_0$. Similarly, when the drift in region II is averaged over region II, then the average drift will be zero. However, the average drift in Region III will not be zero. The effect of the drift in region III can be expressed as follows:

$$\langle \mathbf{V}_{\mathrm{III}} \rangle = \frac{1}{\pi a'^2}\int_{\mathrm{III}} d\mathbf{x}'\, \mathbf{V}_{\mathrm{III}} = \frac{-1}{\pi a'^2}\left(\int_{\mathrm{III}} d\mathbf{x}' \frac{a^2\omega_0}{|\mathbf{x}' - \mathbf{X}_0|^2}(\mathbf{x}' - \mathbf{X}_0)\right)\times\hat{b}. \tag{32}$$

Assuming $\Delta \equiv |\mathbf{\Delta}| = |\mathbf{X}_0 - \mathbf{X}_0'| \ll a' \sim b$ and $a' \gg a + 2\Delta$, then $|\mathbf{x}' - \mathbf{X}_0| \cong a'$, and the above equation can be written as follows:

$$\langle \mathbf{V}_{\mathrm{III}} \rangle \cong \frac{-\omega_0}{\pi a'^2}\left(\frac{a}{a'}\right)^2\left(\int_{\mathrm{III}} d\mathbf{x}'(\mathbf{x}' - \mathbf{X}_0)\right)\times\hat{b}. \tag{33}$$

In Fig. 4 it can be seen that the above drift will be in the $\mathbf{\Delta}\times\hat{b}$ direction and will be the following:

$$\langle \bar{V}_{\mathrm{III}} \rangle \cong \frac{-\omega_0}{\pi a'^2}\left(\frac{a}{a'}\right)^2\left(\int_0^{2\pi} a'^2\, d\theta\,(1 + \cos\theta)\cos\theta\right)(\mathbf{\Delta}\times\hat{b}) = -\omega_0(a/a')^2(\mathbf{\Delta}\times\hat{b}). \tag{34}$$

Using the above equation and the previously mentioned assumptions, then the particle drift equations can be averaged to find the background beam motion and the accelerated beam motion. The resulting equations are the following when $N \ll N'$:

$$\dot{X}_0 = -\omega_1 Y_0 + \omega_2 Y_0', \qquad \dot{Y}_0 = \omega_1 X_0 - \omega_2 X_0' - U, \tag{35}$$

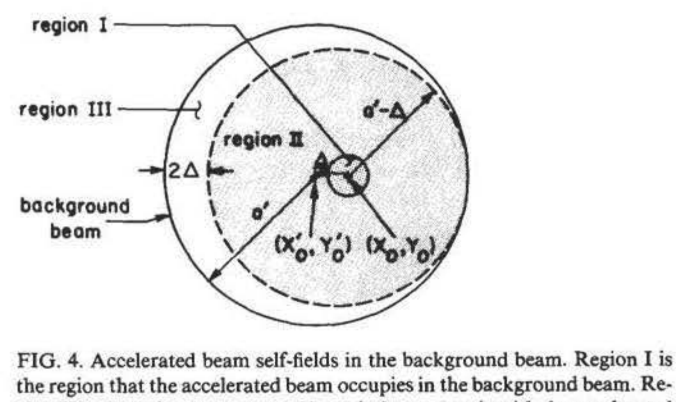

FIG. 4. Accelerated beam self-fields in the background beam. Region I is the region that the accelerated beam occupies in the background beam. Region II is the region encompassed by a circle concentric with the accelerated beam's center and touching the edge of the background beam. Region III is the remainder of the background beam.

$$\dot{X}'_0 = -\omega_3 Y'_0 + \omega_4 Y_0,$$
$$\dot{Y}'_0 = \omega_3 X'_0 - \omega_4 X_0 - U', \tag{36}$$

where

$$\omega_1 \cong \omega'_0, \quad \omega_2 \cong \omega'_0\left[1 - \left(\frac{a'}{b}\right)^2\right], \quad \omega_3 \cong \omega'_0\left(\frac{a'}{b}\right)^2,$$

$$\omega_4 \cong \omega_0\left[\left(\frac{a}{a'}\right)^2 - \left(\frac{a}{b}\right)^2\right],$$

$$U = -\frac{B_{y0}}{B_{z0}}\langle V_\parallel\rangle + \frac{\langle V_\parallel^2\rangle + \frac{1}{2}\langle V_\perp^2\rangle}{\Omega_z R},$$

$$U' \cong \frac{\langle V_\parallel'^2\rangle + \frac{1}{2}\langle V_\perp'^2\rangle}{\Omega_z R}.$$

This analysis indicates that the background beam motion will be coupled to the accelerated beam motion. In order to find the oscillation frequencies, a normal mode analysis must be used. To accomplish this the above guiding center equations will be expressed in the harmonic oscillator form:

$$\ddot{X}_0 = -\Omega_1^2 X_0 + \Omega_2^2 X'_0, \tag{37}$$

$$\ddot{Y}_0 = -\Omega_1^2 Y_0 + \Omega_2^2 Y'_0, \tag{38}$$

$$\ddot{X}'_0 = \Omega_3^2 X_0 - \Omega_4^2 X'_0, \tag{39}$$

$$\ddot{Y}'_0 = \Omega_3^2 Y_0 - \Omega_4^2 Y'_0, \tag{40}$$

where

$$\Omega_1^2 = \omega_1^2 + \omega_4\omega_2 \cong \omega_0'^2,$$
$$\Omega_2^2 = \omega_2(\omega_1 + \omega_3) \cong \omega_0'^2[1 - (a'/b)^4],$$
$$\Omega_3^2 = \omega_4(\omega_1 + \omega_3) \cong \omega'_0\omega_0[1 + (a'/b)^2][(a/a')^2 - (a/b)^2], \tag{41}$$
$$\Omega_4^2 = \omega_3^2 + \omega_2\omega_4 \cong \omega_0'^2(a'/b)^4.$$

Assuming oscillations of the form $\exp(i\omega t)$ the eigenfrequencies can be found. They are given by the following equation:

$$(\omega^2 - \Omega_1^2)^2(\omega^2 - \Omega_4^2)^2 = \Omega_3^4\Omega_2^4. \tag{42}$$

Since $\Omega_3^2/\Omega_1^2, \Omega_3^2/\Omega_2^2$, and $\Omega_3^2/\Omega_4^2 \ll 1$, then the above equation has solutions $\omega = \pm\Omega_1 + \delta\omega_1$ and $\omega = \pm\Omega_4 + \delta\omega_4$, where $\delta\omega_1$ and $\delta\omega_4 \ll \omega$. When $\omega = \pm\Omega_1 + \delta\omega_1$ the above equation can be approximated as

$$2\,\delta\omega_1\Omega_1(\Omega_1^2 - \Omega_4^2) \cong \pm\Omega_3^2\Omega_2^2,$$

or

$$\delta\omega_1 \cong \frac{\pm\Omega_3^2\Omega_2^2}{2\,\Omega_1(\Omega_1^2 - \Omega_4^2)}. \tag{43}$$

When $\omega = \pm\Omega_4 + \delta\omega_4$ then Eq. (42) becomes

$$\delta\omega_4 \cong \frac{\pm\Omega_3^2\Omega_2^2}{2\,\Omega_4(\Omega_1^2 - \Omega_4^2)}. \tag{44}$$

Therefore, the eigenfrequencies are given by the following:

$$\omega \cong \begin{cases} \pm\omega'_0 \pm \frac{1}{2}\omega_0\left[1 + \left(\frac{a'}{b}\right)^2\right]\left[\left(\frac{a}{a'}\right)^2 - \left(\frac{a}{b}\right)^2\right] \\ \pm\omega'_0\left(\frac{a'}{b}\right)^2 \pm \frac{1}{2}\omega_0\left[1 + \left(\frac{a'}{b}\right)^2\right] \\ \quad\times\left[\left(\frac{a}{a'}\right)^2 - \left(\frac{a}{b}\right)^2\right]\left(\frac{a'}{b}\right)^{-2}. \end{cases} \tag{45}$$

In the betatron, high and low oscillation frequencies were observed. The low frequency corresponds to a beat frequency which will appear on probes since they will observe a combination of high frequencies that differ by a small frequency. The low frequency is consistent with the line density in the experiment which was obtained by current measurements. This can be seen in Eq. (45) since the difference in frequency is approximately $\omega_0(a/a')^2 = 2Nec/B_{z0}a'^2$ for $a' \sim 4$ cm and $b = 5$ cm. This indicates that the accelerated beam's line density should be obtainable from the low frequency measurements:

$$N \cong \omega_s(B_{z0}a'^2/2ec), \tag{46}$$

where ω_s is the low oscillation frequency observed in the experiment. In the UCI modified betatron a typical set of data had $B_{z0} \approx 4$ kG, and $\omega_s \approx 6\times 10^6\ \text{sec}^{-1}$. If the radius of the background beam is taken to be 4 cm, which was the distance between the injector and the center of the torus, then the line density should be about $1.3\times 10^{10}\ \text{cm}^{-1}$ via Eq. (46). In the experiment the beam current (I) was about 100 A so that the measured line density was about $2\times 10^{10}\ \text{cm}^{-1}$, which is close to the value predicted by Eq. (46).

The time-averaged displacements of the background and accelerated beams can also be obtained from Eqs. (35) and (36). These equations indicate that on average the accelerated beam will be displaced to a point $(\bar{X}_0, \bar{Y}_0)$ and the background beam will be displaced to a point $(\bar{X}'_0, \bar{Y}'_0)$, which are given by the following:

$$\bar{X}_0 \cong \left\{\frac{\langle V_\parallel^2\rangle}{R\Omega_z} - \frac{\langle V_\parallel\rangle B_{y0}}{B} + \frac{\langle V_\perp^2\rangle}{2R\Omega_z} + \frac{\langle V_\perp'^2\rangle}{2R\Omega_z}\right. \left.\times\left[1 - \left(\frac{a'}{b}\right)^2\right]\left(\frac{b}{a'}\right)^2\right\}(\omega'_0)^{-1}, \tag{47a}$$

or

$$\omega'_0(\bar{X}_0 - \bar{X}'_0) \cong \frac{\langle V_\parallel^2\rangle + \frac{1}{2}\langle V_\perp^2\rangle}{\Omega_z R} - \frac{\langle V_\parallel\rangle\Omega_y}{\Omega_z} - \frac{2N'ec}{b^2 B_{z0}}\bar{X}'_0, \tag{47b}$$

also

$$\bar{X}'_0 \cong \frac{\langle V_\perp'^2\rangle/2R\Omega_z}{\omega'_0(a'/b)^2}, \tag{48}$$

$$\bar{Y}_0 \text{ and } \bar{Y}'_0 \cong 0. \tag{49}$$

Equation (47b) shows that the equilibrium accelerated beam position $(\bar{X}_0)$ is the point where the drift from the background beam electric field [shown on the left-hand side of Eq. (17b)] cancels the drifts from the curvature of the magnetic fields, particles following the betatron field, and the electric field induced on the wall from the shift in background beam position. Since the electric field from the background beam is relatively large, a large mismatch on the right-hand side of Eq. (47b) can be tolerated without a large accelerated beam displacement.

When the equation for the average X displacement of the accelerated beam is compared with the single beam case, Eq. (17a), it can be seen that the two-beam case has a smaller displacement for a given mismatch in the betatron condition, i.e., $\Omega_y R \neq \langle V_\parallel \rangle$. This can be interpreted as the quasiconfined particles providing fields that confine the accelerated beam. Quantitatively, these fields are much larger than the image field of the accelerated beam. Specifically, if the quantity $N' \equiv n'\pi a'^2$ is identified by associating the fast oscillation frequency in the experiment with ω_0', as was indicated by Eq. (45), then for the two-beam case the accelerated beam has a predicted displacement of about -6 cm with the previously mentioned data. Since 5 cm is the minor radius of the torus, the two-beam theory corresponds quite favorably with the experiment on the question of when the beam hits the wall.

In the experiment it was also observed that the accelerated beam would hit the wall in about 20 μsec if the injector was turned off. Since it is expected that the background beam will essentially fill the torus, background particles will constantly be lost. If injection is stopped, the background beam particles will not be replaced, resulting in the loss of the background beam and thereby the accelerated beam. The lifetime of the background beam can be estimated by assuming an equilibrium between the loss of background particles and the injection of new particles. Assuming this, the characteristic lifetime of the background beam is $\tau = 2\pi RN'/(I/e) \approx 20\,\mu$sec, where I is the injector current (≈ 2A). Additionally, it is useful to note that the instability that appeared in the single beam model when $s \neq \frac{1}{2}$ is absent here since the oscillation frequency does not significantly depend on the betatron field.

IV. COMPARISON OF THE PARAXIAL AND GUIDING CENTER TREATMENTS

Both the paraxial and guiding center treatments are based on the force equations for a beam particle. The exact force equations are the following:

$$\frac{d}{dt}(\gamma m v_x) = -\frac{\gamma m v_z^2}{(R-x)} + eE_x + \frac{e}{c}(v_y B_z - v_z B_y), \tag{50}$$

$$\frac{d}{dt}(\gamma m v_y) = eE_y + \frac{e}{c}(v_z B_x - v_x B_z). \tag{51}$$

In the paraxial treatment $V_z^2 \gg V_\perp^2$, all the fields are expanded in powers of x and y and only those terms that are constant or proportional to x, y, $\dot{x}$, $\dot{y}$, $\ddot{x}$, and $\ddot{y}$ are kept. By making the above assumptions and averaging the above equations over all beam particles the following beam equations are obtained when $V_z \cong c$:

$$\ddot{X}_0 = F + \omega_x^2 X_0 + \Omega_z \dot{Y}_0, \tag{52}$$

$$\ddot{Y}_0 = \omega_y^2 Y_0 - \Omega_z \dot{X}_0, \tag{53}$$

where

$$\begin{aligned} \omega_x^2 &= (\omega_p^2/2)(a/b)^2 - (c/R)^2 + s\Omega_y(c/R), \\ \omega_y^2 &= (\omega_p^2/2)(a/b)^2 - s\Omega_y(c/R), \\ F &= -c(c/R - \Omega_y). \end{aligned} \tag{54}$$

The above indicates oscillations about an equilibrium. The equilibrium position $(\bar{X}_0, \bar{Y}_0)$ is given by the following:

$$\bar{X}_0 = \frac{c[(c/R) - \Omega_y]}{(\omega_p^2/2)(a/b)^2 - (c/R)^2 + s\Omega_y(c/R)}, \tag{55}$$

$$\bar{Y}_0 \cong 0, \tag{56}$$

when the betatron condition is satisfied, $\bar{X}_0$ becomes zero, and there is no average deflection of the beam. The oscillation frequencies can be obtained by assuming X_0 and Y_0 are proportional to $\exp(-i\omega t)$ in which case ω is the following:

$$\begin{aligned} \omega^2 = -\tfrac{1}{2}\{&(\omega_x^2 + \omega_y^2 - \Omega_z^2) \\ &\pm [(\omega_x^2 + \omega_y^2 - \Omega_z^2)^2 - 4\omega_x^2\omega_y^2]^{1/2}\}. \end{aligned} \tag{57}$$

In the above it can be seen that if for a particular B_y, ω_x^2 and ω_y^2 are of different signs, then one root of ω is imaginary and there will be an instability. This corresponds to the instability shown in Sec. II with the one-beam guiding center equations. Also, it can be seen that assuming $\Omega_z^2 \gg \omega_p^2$, there are two basic frequencies predicted by the above; one is around the cyclotron frequency and the other around the diocotron frequency.[2] This is also similar to the guiding center treatment except that the cyclotron frequencies are absent since the cyclotron oscillations are averaged out. By comparing the above paraxial equations to the one-beam guiding center equations, it can be seen that the results of these treatments differ. The major differences are that the guiding center treatment includes effects from the perpendicular energy, and the paraxial treatment explicitly includes the cyclotron motion. It can be seen that in situations where there are nonparaxial particles, the guiding center treatment is appropriate.

In summary, beam equilibrium and oscillations in a modified betatron can be described using a guiding center approach. Two cases were examined, one where all the particles in the accelerator would be accelerated, and the other where there would be a background of quasiconfined particles in addition to the accelerated beam. The data collected with the UCI Modified Betatron are consistent with the two beam case. It was found that a large number of quasiconfined particles create electric fields that cause drifts that can stabilize the accelerated beam. When compared with the one-beam case, the quasiconfined particle beam has larger electric fields so that a larger mismatch in the betatron condition can be tolerated before the accelerated beam would hit the wall.

ACKNOWLEDGMENTS

This paper is based on the Ph.D. thesis of G. A. Roberts at University of California, Irvine.

This work was sponsored by the Office of Naval Research.

[1]G. Barak and N. Rostoker, Phys. Fluids **26**, 856 (1983).
[2]C. A. Kapetanakos, P. Sprangle, D. P. Chernin, S. J. Marsh, and I. Haber, Phys. Fluids **26**, 1634 (1983).
[3]F. Sandel, F. Mako, and C. A. Kapetanakos, Bull. Am. Phys. Soc. **28**, 1146 (1983).
[4]J. D. Daugherty, J. E. Eninger, and G. S. Janes, Phys. Fluids **12**, 2677 (1969).
[5]B. Mandelbaum, H. Ishizuka, A. Fisher, and N. Rostoker, *Proceedings of the 5th International Conference on High Power Electron and Ion Beam Research and Technology*, San Francisco, California, 1983, p. 476.
[6]D. Chernin and P. Sprangle, Part. Accel. **12**, 85 (1982).
[7]W. Clark, P. Korn, A. Mondelli, and N. Rostoker, Phys. Rev. Lett. **37**, 592 (1976).